TURBO-15-1088

Bleed-Induced Distortion in Axial Compressors

S.D. Grimshaw, G. Pullan
Whittle Laboratory
University of Cambridge
1 JJ Thomson Avenue
Cambridge, CB3 0DY, UK
Email: sdg33@cam.ac.uk

T. Walker
Mitsubishi Heavy Industries Ltd
Takasago Research and Development Centre
Takasago, Japan

ABSTRACT

In this paper, the influence of non-uniform bleed extraction on the stability of an axial flow compressor is quantified. Non-uniformity can be caused by several geometric factors (for example, plenum chamber size or number of off-take ducts) and a range of configurations is examined experimentally in a single stage compressor. It is shown that non-uniform bleed leads to a circumferential distribution of flow coefficient and swirl angle at inlet to the downstream stage. The resultant distribution of rotor incidence causes stall to occur at a higher flow coefficient than if the same total bleed rate had been extracted uniformly around the circumference. A connection is made between the analysis of non-uniform bleed extraction and the familiar "DC_θ" criterion used to characterize inlet total pressure distortion. The loss of operating range caused by the non-uniform inlet flow correlates with the peak sector-averaged bleed non-uniformity for all the bleed configurations tested.

INTRODUCTION

In axial compressors for aero-engines and land-based gas turbines, it is common for a proportion of the mass flow entering the compressor to be removed part-way through the device. This "bleed flow" is needed for a variety of requirements including supplying the combustor and turbine with cooling air and improving the stage matching of the compressor during operation at off-design conditions. The fraction of main annulus flow bled from a particular stage can vary greatly from less than 5% at the design point to more than 10% during machine start up. Several arrangements of slots and holes have been employed to remove the bleed air through the compressor casing [1, 2]. Such geometry is either axisymmetric or periodic

on the length scale of a blade pitch. After passing through the casing, however, the bleed air will typically enter a plenum chamber and then off-take ducts. These configurations are not axisymmetric but are periodic on a length scale of the order of the circumference. The influence of this asymmetry on the circumferential uniformity of the bled flow, and on the stability of the compressor, is the subject of this paper.

It is useful to divide discussion of the impact of bleed on compressor stability into three parts: the flow field associated with "uniform bleed"; the flow field associated with "non-uniform bleed"; and the connection between flow field and stability. We will classify bleed as uniform when the variations in bleed that are periodic on a length scale of the order of the machine circumference are small.

Studies of uniform bleed have been performed using computations of compressors [3, 4] and also using linear cascade experiments [1, 2, 5]. Wellborn and Koiro [4] show that, when operating the stage downstream of the bleed at fixed rotor inlet flow coefficient, the spanwise distribution of axial velocity is unaffected by increasing the bleed rate from 1% to 5% of the mainstream flow. This result suggests that a passage-averaged one-dimensional treatment is sufficient to model the performance of the compressor.

Non-uniform bleed has been investigated by Gomes *et al.* [6], and Gomes and Schwarz [7], using an annular cascade with a row of stator blades upstream of a bleed system. The bleed system was designed to be configurable so the shape of the bleed slot, size of plenum chamber and number and circumferential distribution of its off-take ducts, could be changed. It is shown that an asymmetric bleed system configuration gives a circumferentially non-uniform pressure at the hub, below the bleed slot, and this is linked to the non-uniform bleed extraction of flow from the main annulus flow. It is suggested that this may have a negative effect on the compressor aerodynamics though this is not explained further and cannot be tested since the experiment does not include a stage downstream of the bleed slot.

Di Mare *et al.* [8] conducted an unsteady CFD study on the effect of bleed flows of 3.6% and 20% on flutter and forced response in axial compressors. They show that increasing bleed rate from 3.6% to 20% moves the downstream rotor operating point up and to the left on its characteristic: the normalised mass flow function reduces by 0.08 and the normalised pressure ratio increases by 0.025. They also show that the 3.6% bleed case only changes the pitchwise-averaged Mach number downstream of the bleed extraction in the outer 20% of span.

There are no known reports of the effect of non-uniform bleed on compressor stability but there is a clear connection to studies of inlet total pressure distortion. Reid [9] shows that an inlet total pressure distortion reduces the operating range of a compressor but that a distortion of spatial extent less than a critical sector size has little effect. This result led to the definition of a distortion parameter DC_θ that characterizes the distortion as the largest drop in total pressure (compared to the average) in any sector of angle θ. The critical angle θ is compressor dependent but is usually between 60 degrees and 120 degrees.

The contributions of this paper are a qualitative description of the compressor flow field in the presence of non-uniform bleed and a quantitative connection between non-uniform bleed distribution and change in stability margin of the downstream stage. We will show that the change in flow coefficient at stall between non-uniform bleed and uniform bleed (at the same total bleed rate) correlates with the peak bleed rate non-uniformity averaged over a 90 degree sector.

The paper is organised as follows: we first describe our conceptual view of the influence of non-uniform bleed. The test

compressor and measurement approach is then given. Data from the compressor are discussed in the order of uniform bleed, non-uniform bleed and stability. Finally, we show that a critical sector approach, analogous to that developed for inlet total pressure distortions, can be used to characterize the response of the compressor to this non-uniform flow.

NOMENCLATURE

c_x	Axial chord
r_{mid}	Mid-height radius
P	Pressure
P_{01}	Inlet stagnation pressure
U	Mid-height blade speed
V_x	Axial velocity
α	Flow angle
α_{rel}	Relative flow angle
ρ	Density
μ	Dynamic viscosity
ϕ	Flow coefficient $= V_x/U$
ψ	Total-to-static pressure rise coefficient $= \frac{P_{exit}-P_{01}}{\frac{1}{2}\rho U^2}$

CONCEPTUAL APPROACH

In general, bleed is extracted from an embedded stage of an axial compressor. Of interest is the stability of the stage immediately downstream of the bleed. The stability of this stage is governed by the flow coefficient at rotor inlet (downstream of the bleed). If the flow into the rotor is reduced sufficiently the compressor will stall either via "modes" (if the stage reaches the peak of its total-to-static pressure rise characteristic) or "spikes" (if stall occurs, due to high rotor incidence, on the negative slope of the characteristic). The test compressor in the present work exhibits spike-type stall inception so that rotor incidence determines when the stage stalls.

To simplify the problem, the geometry considered is a single stage compressor with a bleed slot immediately upstream. Typical of the mid-to-rear stages where bleed is generally employed, the test compressor used in this report has a high hub-to-tip radius ratio of 0.75. This means that uniform bleed leads to low meridional curvature of the axisymmteric streamsurfaces, so that the effect of bleed on the downstream stage is expected to be predominantly one-dimensional (as seen in [4]). As the bleed rate is increased, the downstream stage operates at a lower flow coefficient (closer to stall) on its characteristic.

Non-uniform bleed extraction through the slot will result in a circumferentially non-uniform distribution of incidence on to the downstream rotor. We note here that the link between bleed extraction distribution and incidence distribution will be different when stages are present upstream of the bleed (for example, the static pressure distortion created by the non-uniform bleed would cause the upstream stage to deliver a non-uniform total pressure). However, the connection between the circumferential distribution of rotor incidence and the stability of the downstream stage - the subject of this paper - does not depend on the presence of stages upstream of the bleed slot.

LOW SPEED COMPRESSOR WITH BLEED

The experiments described in this paper were performed with a one-stage, axial-flow, test compressor with inlet guide vanes (IGVs) and a high hub-to-tip radius ratio. The compressor design is typical of the rear stages of a land-based gas turbine. Details are given in Table 1.

Hub-to-tip radius ratio	0.75
Design $\phi = V_x/U$	0.43
Design $\psi = (p_2 - p_{01})/(0.5\rho U^2)$	0.48
Tip speed Mach number	0.23
Rotor Re$= (\rho V_1^{rel} c)/\mu$	1.6×10^5
Rotor tip gap	1.7% c_x (=0.4 mm)
Rotor blade count	58
Stator blade count	60
Casing diameter	0.51m

(a) Low-speed test compressor

Large ($\Delta x \times \Delta r$, volume)	146×79mm, 0.0266m^3
Medium ($\Delta x \times \Delta r$, volume)	86×44mm, 0.0084m^3
Small ($\Delta x \times \Delta r$, volume)	86×10mm, 0.0018m^3

(b) Plenum chamber geometries

Table 1: Data for low-speed compressor with bleed

Bleed air is extracted from the compressor through a bleed system which consists of an axisymmetric bleed slot, an annular plenum chamber and one or more off-take ducts. The off-take ducts are connected to orifice plates and control valves which measure and regulate the bleed mass flow rate. These are attached to vacuum pumps which provide the suction to draw air through the bleed system. The bleed slot design is representative of an industrial gas turbine and the volume of the plenum chamber can be changed. Details of the three plenum chambers tested are given in Table 1. The number and location of the off-take ducts can also be changed and tests were performed with four equi-spaced off-take ducts, two off-take ducts with a variety of circumferential separations, and one off-take duct.

Five measurement stations are referred to in the paper and these are shown in Fig. 1 which also shows the layout of the rig.

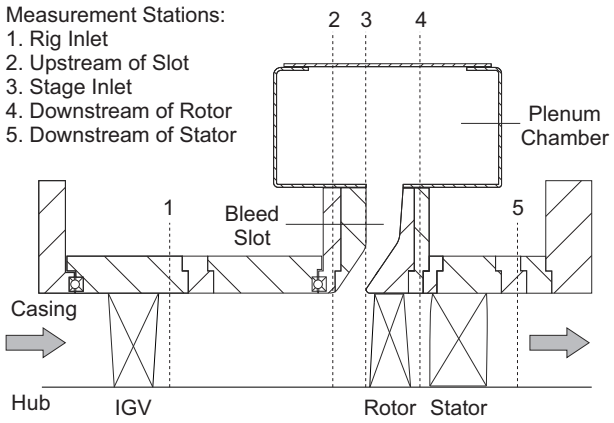

Fig. 1: Meridional view of test compressor showing measurement planes

Total-to-static pressure rise is measured using Pitot tubes upstream of rig inlet and static pressure tappings downstream of the stators. An inlet calibration is used to obtain the rig inlet flow coefficient, ϕ_{rig}, from the Pitot tubes and rig inlet static tappings. The stage inlet flow coefficient, ϕ_{stage}, is obtained by subtracting the measured bleed mass flow rate from the rig inlet mass flow rate. The measured stalling flow coefficient was obtained by averaging ten stall events. The standard deviation of a typical set of ten stalling flow coefficients was found to be 0.15%.

Five hole probe area traverses were performed with an automated traversing system. In all cases the traverses are over one stator pitch and contain 21 evenly spaced pitchwise points and 21 radial points clustered towards the end walls. For circumferentially non-uniform bleed traverses the relative position of the off-take duct and the traverse location were changed by moving the off-take duct to different circumferential positions.

To provide data to confirm the stall inception route, six high frequency pressure transducers, spaced equally around the casing, are mounted 13% of axial chord upstream of the rotor tip. For the measurements in this paper the signal is logged at 80kHz and this gives 26.7 data points per blade passing. This output is logged continuously with a buffered logging system and 1 second of data is recorded when stall occurs.

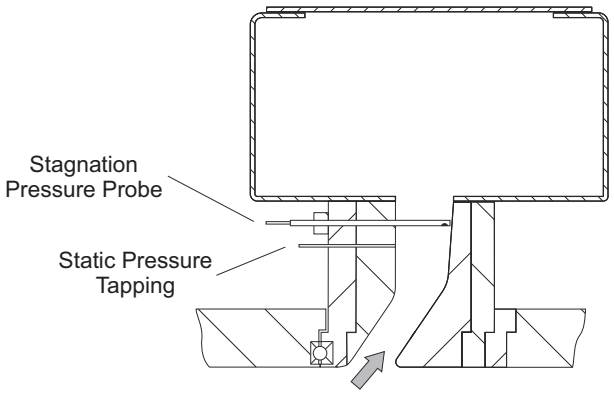

Fig. 2: Detail of bleed slot instrumentation

The local bleed mass flow rate is measured in the bleed slot using 16 equally spaced pairs of static pressure tappings and stagnation pressure probes. Figure 2 shows the location of the static pressure tapping and stagnation pressure probe in the bleed slot. The total pressure probe is rotated to align with the flow and from this the flow angle in the slot is obtained. The probes are calibrated for bleed mass flow rate during uniform bleed tests. The calibration is then used, along with the flow

angle, to calculate the local radial bleed rate through the slot at each of the 16 circumferential locations.

PRESENTATION OF RESULTS

Results from the compressor experiments are presented in three parts. First, data from uniform bleed extraction at a range of bleed rates are used to characterise the response of the compressor to bleed. Second, results from one non-uniform bleed configuration (4.1% bleed, Small Plenum, one off-take duct) are presented to develop a conceptual picture of the influence of non-uniform bleed on the circumferential distribution of the stage inlet flow. The analysis of the compressor flow fields, for both uniform and non-uniform bleed, is split into passage-averaged (no spanwise variations) and pitch-averaged approaches. In the final part, a peak sector-averaged bleed non-uniformity metric is proposed and shown to correlate with the reduction in stall margin from the equivalent uniform bleed case for all the configurations tested.

UNIFORM BLEED

To provide a stepping stone toward the discussion of non-uniform bleed, we first present the effect of uniform bleed on compressor performance. A second motivation is that bleed extraction will be close to uniform in many machines and it is therefore useful to understand the effect of uniform bleed extraction on downstream stage performance.

The bleed system is set up with the Large Plenum chamber and four equi-spaced off-take ducts. The passage-averaged response of the stage is first examined using total-to-static pressure rise characteristics at different bleed rates. Spanwise distributions of the flow are then obtained by pitch-averaging the data from area traverses (taken over a 1 pitch $\times$ 1 span measurement window) at the five measurement stations. Finally, the route to stall is investigated and the effect of bleed rate on the stall point quantified.

Passage-averaged analysis

Figure 3 shows the rig inlet total-to-static pressure rise (station 1 to station 5) characteristics for bleed rates of 0%, 2.1%, 4.1% and 6.2%. As bleed rate is increased the total-to-static pressure rise increases for a given rig inlet flow coefficient, ϕ_{rig} because the stage inlet flow coefficient, ϕ_{stage}, is reduced. The same cases, but with stage inlet total-to-static pressure rise (station 3 to station 5) plotted against the stage inlet flow coefficient, ϕ_{stage}, are shown in Fig. 4. The characteristics now collapse toward a single line, illustrating that the compressor response is dominated by the passage-averaged flow at rotor inlet. However, the stage inlet flow coefficient at stall varies by 4% indicating that stall inception is governed by spanwise flow redistribution, and changes in rotor tip incidence, that are not accounted for in a passage-averaged analysis.

Pitch-averaged analysis

Figure 5 shows spanwise distributions of pitch-averaged flow coefficient for bleed rates 0%, 2.1%, 4.1% and 6.2% at a fixed stage inlet flow coefficient $\phi_{stage} = 0.43$. At rig inlet, Fig. 5(a), the flow coefficient increases with increased bleed and this change is uniform across the span. Just upstream of the slot, Fig. 5(b) shows that the bleed extraction causes a radial redistribution of the flow with the flow coefficient increasing more in the outer 30% of span. Figure 5(c) shows traverses at stage inlet, i.e. just downstream of the bleed slot. In this location the passage averaged flow coefficient varies by less than

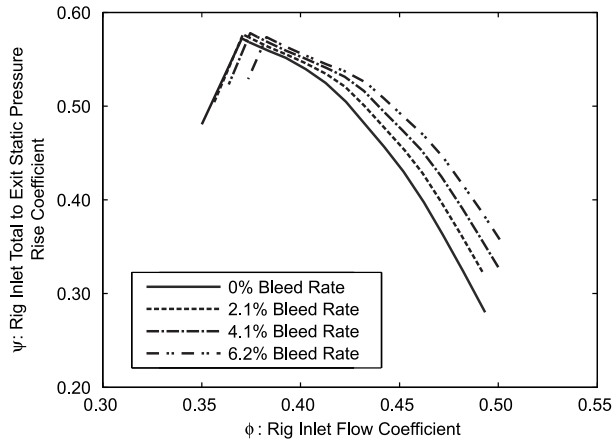

Fig. 3: Rig inlet total-to-static pressure rise characteristic

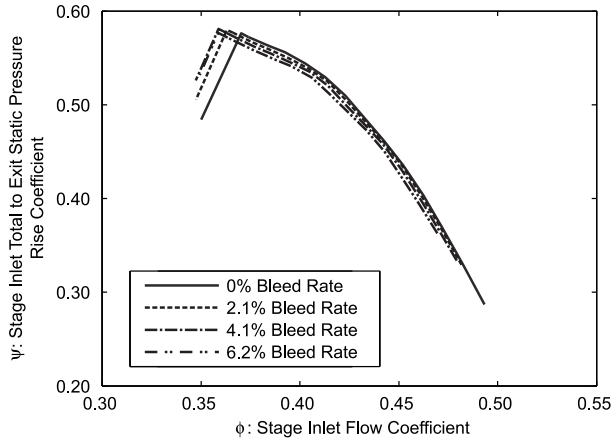

Fig. 4: Stage inlet total-to-static pressure rise characteristic

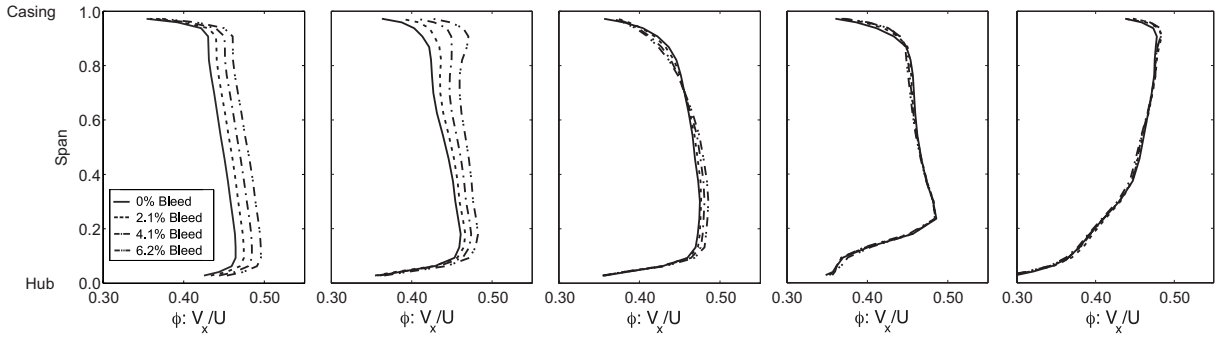

Fig. 5: Spanwise distributions of flow coefficient through the compressor at different bleed rates, fixed $\phi_{stage} = 0.43$

0.8% across the four cases as expected because the stage inlet flow coefficient is fixed. However, as the bleed rate is increased there is a trend for the flow rate in the outer 30% of span to decrease and that over the lower 70% to increase. This change in spanwise profile results in the spread in the pressure rise characteristics of Fig. 4. Downstream of each blade row, Fig. 5(d) and (e), the flow coefficient distributions do not change with varying bleed (at fixed ϕ_{stage}). At lower flow coefficients, the spanwise redistribution of flow due to the bleed extraction follows the same qualitative behaviour as that of Fig. 5.

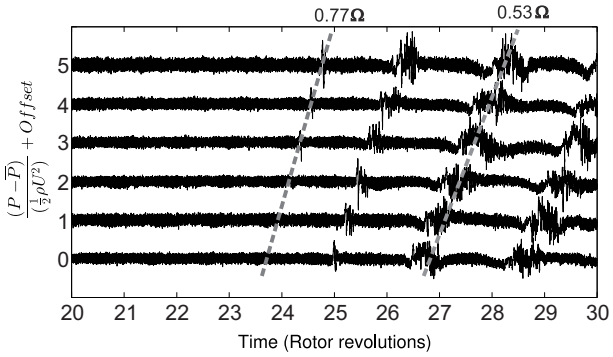

Fig. 6: Unsteady casing pressure transducer traces at rotor inlet at stall

Stall inception

Figure 6 shows the unsteady pressure on the casing 13% of rotor axial chord upstream of the rotor at six equally spaced locations. The bleed rate is 0%. The figure shows that the compressor stalls via spike-type stall inception. The typical spike-type inception pattern can be seen whereby a small disturbance which affects only one or two blade passages appears and propagates around the annulus at approximately 77% of rotor speed. As the disturbances propagate they grow so that more blade passages are affected. After about four rotor revolutions the disturbance has grown into a stall cell which rotates at 53% of rotor speed. The same spike-type stall inception mechanism is observed for all other cases tested, both for uniform and circumferentially non-uniform bleed.

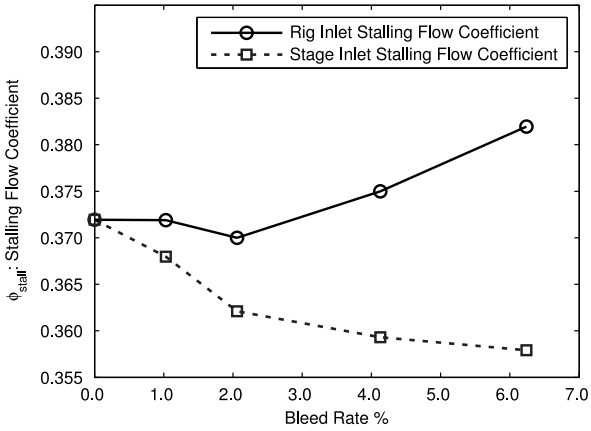

Fig. 7: Rig and stage inlet flow coefficient at stall

Figure 7 shows the rig and stage inlet stalling flow coefficients against bleed rate for circumferentially uniform bleed. The stage inlet flow coefficient at stall reduces (the operating range improves) as bleed rate is increased. Figure 8 shows the flow angle in the rotor relative frame, at stage inlet from 90% to 100% of span at a stage inlet flow coefficient of 0.38 (close to stall). The 0% bleed case has the most negative flow angle in the relative frame and hence highest incidence onto the rotor tip. As the bleed rate is increased, the circumferential velocity component is not affected by the uniform bleed extraction but Fig. 5 shows that, in the outer 30% of span, the axial component of velocity is reduced. This leads to an increased flow angle in the relative frame (reduced incidence). This result is consistent with the 0% bleed case stalling at a higher flow coefficient than for the cases with bleed. Figures 7 and 8 illustrate the sensitivity of the stage inlet flow coefficient at stall to rotor tip incidence.

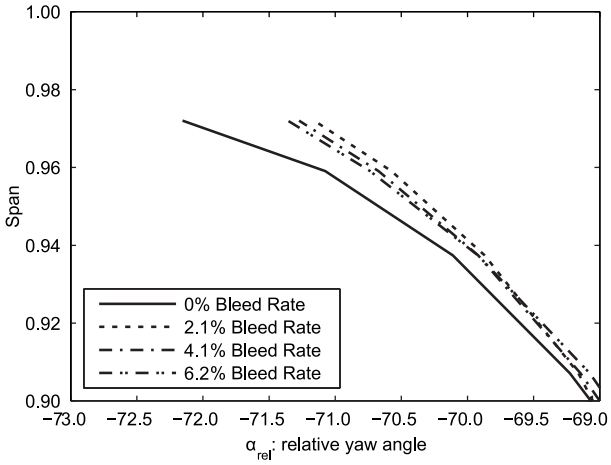

Fig. 8: Spanwise distribution of rotor inlet relative flow angle, near casing, $\phi_{stage} = 0.38$

NON-UNIFORM BLEED

This section describes the effect of circumferentially non-uniform bleed on the flow field with particular attention paid to the flow entering the downstream compressor stage. Measurements from one bleed system configuration (Small Plenum chamber, one off-take duct, 4.1% bleed) are presented. Circumferential distributions of passage-averaged flow quantities are provided and a conceptual description of the flow field proposed that is in accord with the observations. We will show that the non-uniform bleed extraction reduces the operating range of the compressor by increasing the maximum rotor incidence.

Passage-averaged analysis

When the compressor is subject to non-uniform bleed, circumferential averaging can be performed over a range of length scales. Here, we present pressure-rise characteristics obtained by averaging over the whole circumference, and circumferential distributions obtained by passage-averaging individual 5-hole probe traverses performed at several locations around the annulus.

Figure 9 compares the stage inlet total-to-static pressure rise characteristic for the uniform bleed case and the case selected as an example of non-uniform bleed (at the same bleed rate). The non-uniformity of the bleed extraction causes an increase in stage inlet stalling flow coefficient of 3.0%.

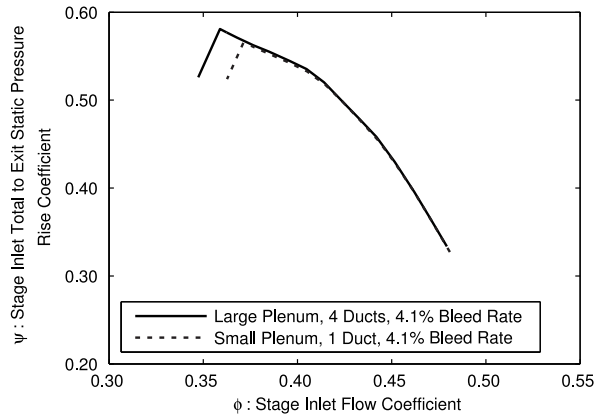

Fig. 9: Stage inlet total-to-static pressure rise characteristics for uniform and sample non-uniform bleed

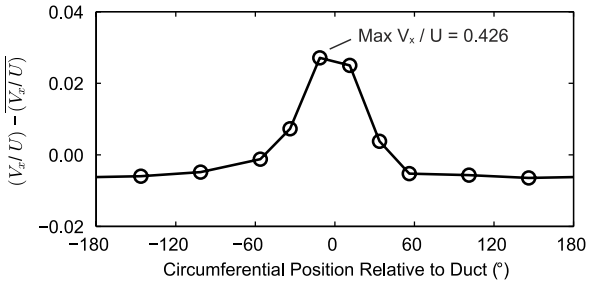

(a) upstream of slot

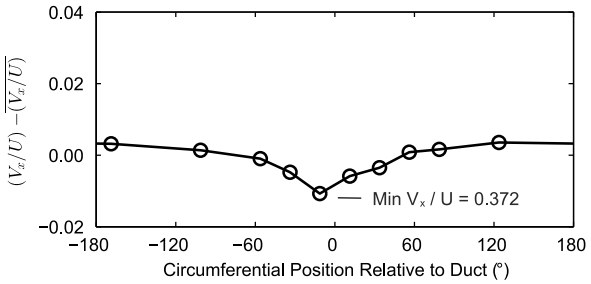

(b) stage inlet

Fig. 10: Variation in local passage-averaged flow coefficient with circumferential position, average $\phi_{stage} = 0.38$

The circumferential distribution of passage-averaged flow coefficient from 10 traverses is shown in Fig. 10. The flow coefficient of the peak non-uniformity is marked on the figures. Upstream of the bleed slot there is an increase in flow at the traverse location closest to the circumferential position of the off-take duct and at stage inlet there is a deficit in flow coefficient at the same circumferential location.

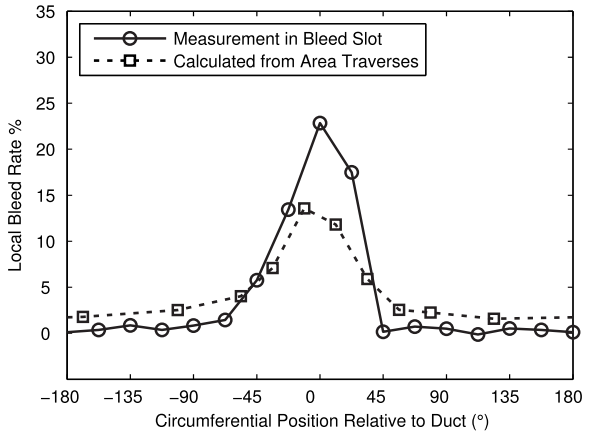

Fig. 11: Comparison of bleed distributions measured in slot and derived from traverse data

The distribution of mass flow extracted through the bleed slot is measured directly using calibrated stagnation pressure probes (Fig. 2) and can also be inferred as the difference between the mass flow distributions upstream and downstream of the slot. Figure 11 shows the distribution of bleed flow obtained by both of these methods. Compared to the bleed slot measurement, the mass flow calculated from the area traverses has a lower, wider peak and some bleed (1.5%) is still extracted 180 degrees away from the off-take duct. These results illustrate the decay of the non-uniform pressure field away from the off-take duct.

The non-uniform pressure field affects the flow angle, as well as the axial velocity, in the main annulus. Rannie and Marble [10] showed that the perturbation distributions of pressure and flow angle are connected by a Cauchy-Riemann relationship and this is evident in the asymmetric absolute frame flow angle distribution at stage inlet plotted in Fig. 12(a). The flow angle in the relative frame, Fig. 12(b), shows a peak rotor incidence perturbation of order 1 degree at a circumferential location offset from the off-take duct by approximately 30 degrees due to the asymmetric absolute flow angle. This localised increase in incidence causes the reduced operating range for the compressor with non-uniform bleed compared to the uniform bleed case at the same bleed rate.

Conceptual description of the passage-averaged flow

The circumferential distributions of passage-averaged axial velocity and flow angle can be explained by considering three cases of increasing complexity: non-uniform bleed extraction with zero net main annulus flow; non-uniform bleed extraction with a main annulus flow; and non-uniform bleed extraction with a main annulus flow and downstream compressor stage.

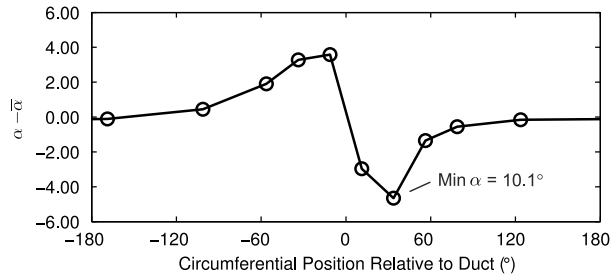

(a) absolute flow angle (deg)

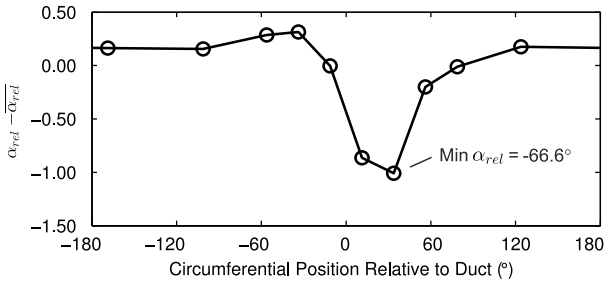

(b) relative flow angle (deg)

Fig. 12: Change in passage-averaged flow angle compared to mean value, $\phi_{stage} = 0.38$

In isolation (zero net main annulus flow), the bleed slot with non-uniform bleed will extract air from upstream and downstream of the slot, Fig. 13. For incompressible flow, the axial velocity perturbations produced by the bleed will be equal and opposite on the upstream and downstream of the slot. The streamlines curve towards the peak in bleed causing an asymmetric circumferential distribution of flow angle.

When the main annulus flow is added, Fig. 14, bleed is no longer extracted from downstream of the slot but the symmetric distribution of the flow coefficient perturbation upstream and downstream of the slot will remain due to the superposition of the bleed slot and uniform annulus flow fields. If the mainstream flow has zero inlet swirl then the flow angle distribution will be asymmetric about the peak bleed close to the slot but tend to zero away from this location in the

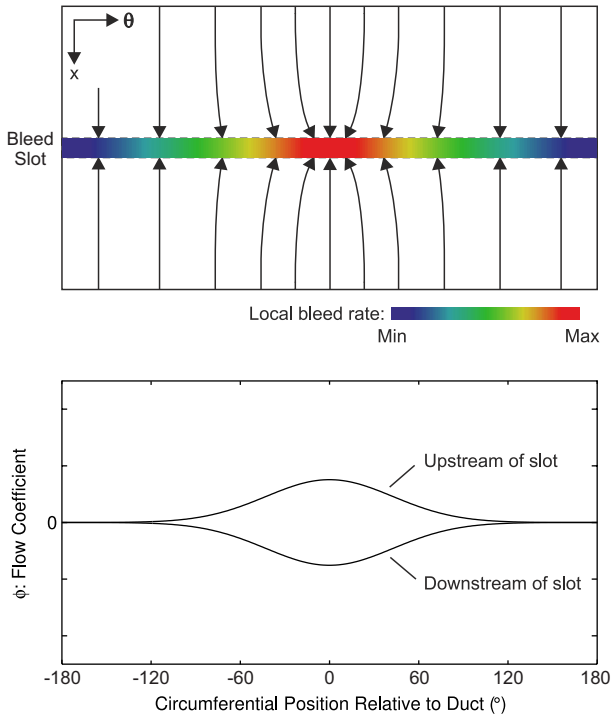

Fig. 13: Flow schematic (top) and flow coefficient distributions for isolated bleed extraction with no net main annulus flow

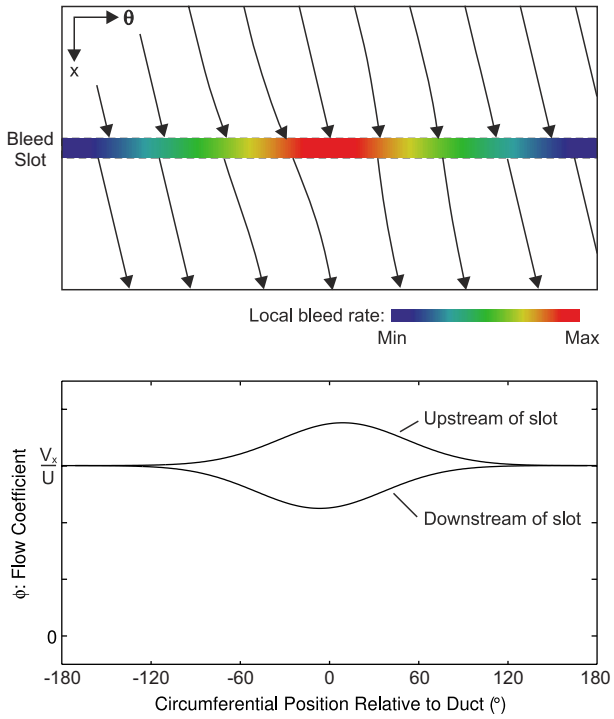

Fig. 14: Flow schematic (top) and flow coefficient distributions for bleed extraction with swirling main annulus flow

upstream and downstream axial directions. With inlet swirl, the flow coefficient distributions upstream and downstream of the bleed slot will become offset in the circumferential direction.

The addition of the downstream compressor stage acts to make the flow coefficient distribution at rotor inlet more uniform. At stage exit the static pressure is circumferentially uniform (the stage outlet flow is at a uniform flow angle and the downstream annulus is constant area, [11]) but the stage inlet flow coefficient is varying and so the compressor operating

point must also vary around the annulus. This means that at stage inlet the compressor imposes its own non-uniform static pressure perturbation on the flow. Specifically, in regions of low inlet flow, the compressor will produce a high static pressure rise so that the static pressure upstream of the stage is reduced and the axial velocity at rotor inlet is increased from the upstream value. The result is that the flow coefficient distribution upstream of the slot becomes more non-uniform and that downstream of the slot becomes more uniform. This effect, and the asymmetric distribution of flow angle, can be seen in the experimental results in Figs. 10 and 12.

Pitch-averaged analysis

The passage-averaged analysis above connects non-uniform bleed extraction and a loss in operating range via the rotor incidence. We now show that the spanwise redistribution of the flow serves to exacerbate this effect by increasing the rotor incidence further in the tip region. Figure 15 shows the circumferential distribution of pitchwise-averaged flow angle in the relative frame at 97.2% of span (i.e. the last radial measurement location in the area traverses). As with the measurements shown in Fig. 12(b) there is a region of increased rotor incidence in the sector close to the off-take duct. At the rotor tip, however, the variation in incidence angle is up to 2 degrees from the mean value, twice that measured using the passage average.

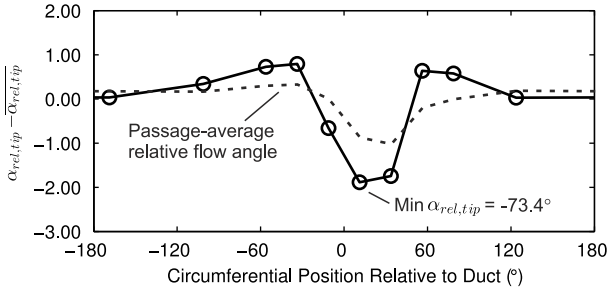

Fig. 15: Flow angle at measurement point closest to casing (97.2% span), $\phi_{stage} = 0.38$

NON-UNIFORM BLEED AND STALL

In this section, the effect of different distributions of non-uniform bleed on the operating range of the downstream stage are collated and a unifying metric proposed. The change in stalling flow coefficient with different bleed system configurations is first presented and a number of sample bleed distributions given. A critical sector concept is developed, similar to that used for inlet total pressure distortion, to characterize the bleed non-uniformity and this parameter is correlated with the reduction in operating range.

Flow coefficient at stall for different bleed system configurations

Figure 16 shows the stage inlet stalling flow coefficient for a range of bleed system configurations against bleed rate. With the Large Plenum chamber and four off-take ducts, increased bleed reduces the stage inlet flow coefficient at which the compressor stalls. For a given bleed rate the stage inlet stalling flow coefficient increases as the number of off-take ducts are reduced from four to one. At a given bleed rate, the operating range is further reduced as the plenum chamber size is

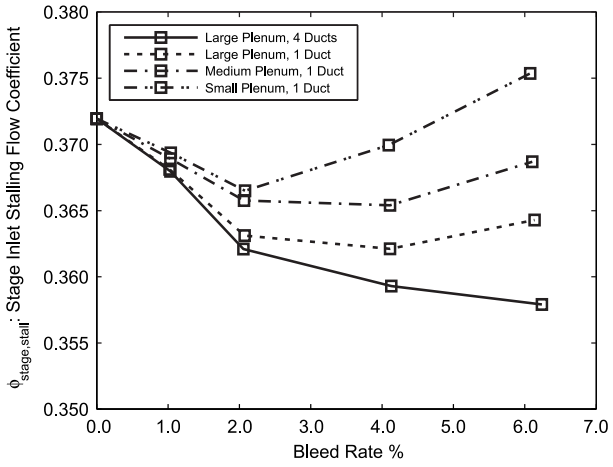

Fig. 16: Stage inlet flow coefficient at stall

decreased. These results can be explained by the increase in bleed non-uniformity caused by reducing the number of off-take ducts and reducing the plenum chamber size. Greater bleed non-uniformity increases the range of incidence angles that the downstream rotor blades move through as they rotate around the annulus. For the rest of this paper the change in operating range for a given bleed distribution is defined as the difference between stalling flow coefficient with that bleed distribution compared to the uniform bleed case (Large Plenum, 4 off-takes) at the same bleed rate.

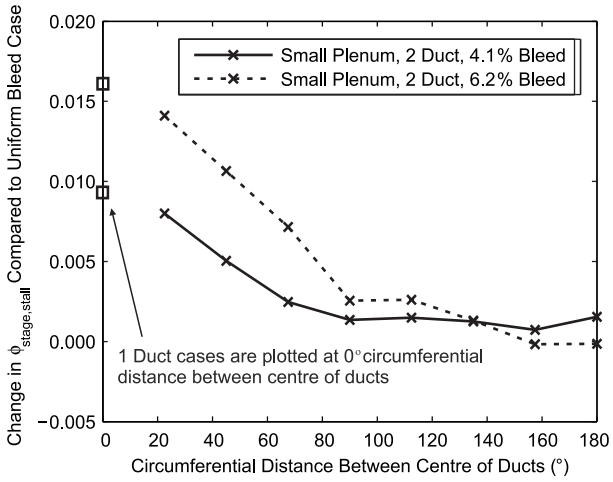

Fig. 17: Variation in stage inlet flow coefficient at stall with angular separation of off-take ducts (2 duct cases)

Figure 17 shows the change in stage inlet stalling flow coefficient against the circumferential distance between the centre of the two ducts. As the off-take ducts are moved closer together, from a separation of 180 degrees to 90 degrees, there is only a small increase in the change in stage inlet stalling flow coefficient. However for a reduction in off-take duct separation from 90 degrees to 22.5 degrees the change in stalling flow coefficient increases. The change in stalling flow coefficient tends towards that of the one off-take duct cases, as expected. This set of experiments is reminiscent of the critical sector angle tests performed by Reid [9] in relation to inlet total pressure distortion. Reid showed that the loss in operating range suddenly increased when a critical sector angle was reached and that one large distorted sector caused a greater loss in operating range than several small sectors with the same total area. In the current work the effect of distortion caused by the individual off-take ducts increases when the ducts are close enough to generate one sector of coalesced peturbations rather than two

separate ones.

Characterization of bleed non-uniformity

We now present and *characterize* the circumferential distributions of bleed that are generated by combinations of bleed rate, plenum chamber size and off-take duct number. Figure 18 shows the local bleed rate against circumferential position for four cases that each extract a bleed rate total of 4.1%. The uniform bleed rate distribution is also shown. For the Small Plenum, one duct case, there is a peak in local bleed rate in the slot close to the duct. The peak has a maximum local bleed rate of 22.9% and width of 135 degrees. In the rest of the slot the local bleed rate is close to 0%. With a Small Plenum and two ducts separated by 90 degrees the bleed distribution now has two peaks, in line with the two off-take ducts. The maximum local bleed rate is 14.2%. The two peaks overlap so the bleed rate does not drop to 0% between them. The width of the combined peaks is 200 degrees. For the Small Plenum with two ducts separated by 180 degrees. The maximum bleed rate is 14.2% and the peaks in local bleed rate are in line with the off-take ducts. Between these peaks the bleed rate falls to nearly zero and the width of each peak is approximately 90 degrees. For the Large Plenum, one duct configuration, the non-uniformity in local bleed rate is less pronounced and the peak bleed rate is 6.9%. In this case the local bleed rate drops to a minimum of 2.9% away from the duct and, as expected, the overall local bleed rate distribution is much less non-uniform than for the Small Plenum chamber cases.

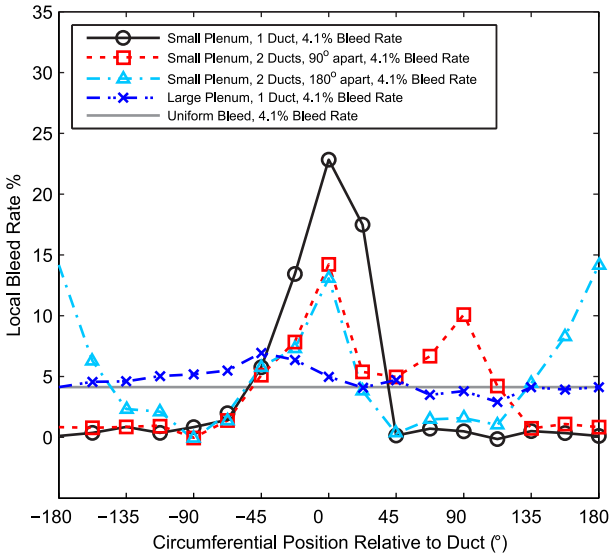

Fig. 18: Variation of local bleed rate in slot with circumferential position relative to off-take duct

It has been shown that the loss in operating range is influenced by the level of non-uniformity and, if there is more than one duct, the spacing between the off-take ducts. These observations point towards a critical sector angle approach and in the spirit of the DC_θ criterion, a method to characterize bleed non-uniformity has been developed. Figure 19 helps to explain how the method is applied. The bleed distribution for the case with 4.1% bleed, a Small Plenum chamber and two off-take ducts with 90 degree separation is shown along with the uniform bleed distribution at that bleed rate. The first step is to calculate the deviation between the measured bleed distribution and the uniform bleed distribution. This is done to reflect how the change in operating range is calculated, i.e. as a difference between the stalling flow coefficients for non-uniform

and uniform bleed cases, at the same bleed rate. The deviation from uniform bleed is then averaged over a fixed sector. The averaging sector is swept over the entire bleed distribution and the result is plotted in Fig. 19 as the 'sector-averaged bleed distribution'. The peak value of this average, i.e. from the sector with the greatest local bleed extraction, provides a parameter for the non-uniformity of the bleed distribution called the peak sector-averaged non-uniformity. The use of the average sector allows the separation between two off-take ducts to be included in the bleed non-uniformity characterization, i.e. bleed from two off-take ducts separated by more than the sector size will result in a lower bleed non-uniformity than bleed from two off-take ducts which are separated by less than the sector size.

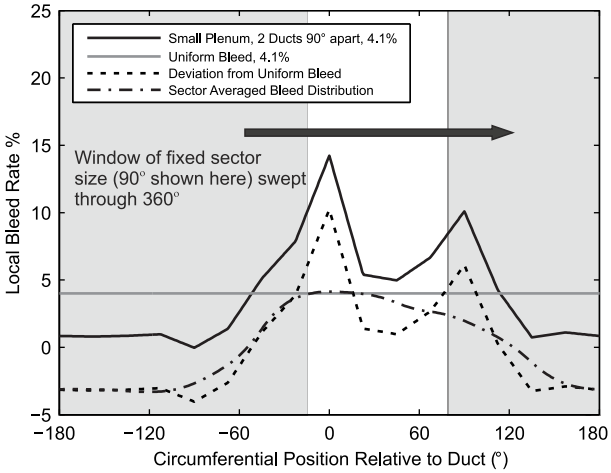

Fig. 19: Obtaining the peak sector-averaged bleed non-uniformity

Effect of bleed non-uniformity on operating range

Local bleed distribution measurements in the slot were taken for 32 different cases with varying bleed rates, plenum chamber sizes, number of off-take ducts and, where relevant, different circumferential separations between the two off-take ducts. The bleed non-uniformity parameter is calculated for each of these cases with sector sizes of 1 to 180 degrees. The change in stage inlet stalling flow coefficient was also measured for each case. Figure 20 shows the coefficient of determination, R^2, for the data best fit line between the change in stage inlet stalling flow coefficient and bleed non-uniformity, for each of the sector sizes. This shows that the best linear fit to the data is found with a sector of 90 degrees (though sector sizes of 60 degrees and 120 degrees give R^2 values within 4% of that obtained with the 90 degree sector). Figure 21 shows the relationship between the bleed non-uniformity and the change in stage inlet stalling flow coefficient for a sector size of 90 degrees. The peak sector-averaged approach for characterising bleed non-uniformity has produced a linear relationship between bleed non-uniformity and loss in operating range for a wide range of different bleed system configurations including two duct cases with different circumferential separations.

The correlation shown in Fig. 21 is useful in an integrated compressor bleed system design process. The impact of different bleed systems on compressor stability can be compared by the peak sector-averaged approach: if two bleed configurations have the same peak sector-averaged bleed non-uniformity, they will have the same influence on compressor stability. In addition, if the reduction in operating range caused by a particular distribution of non-uniform bleed is known, then the change in operating range caused by new bleed distributions can be quantified.

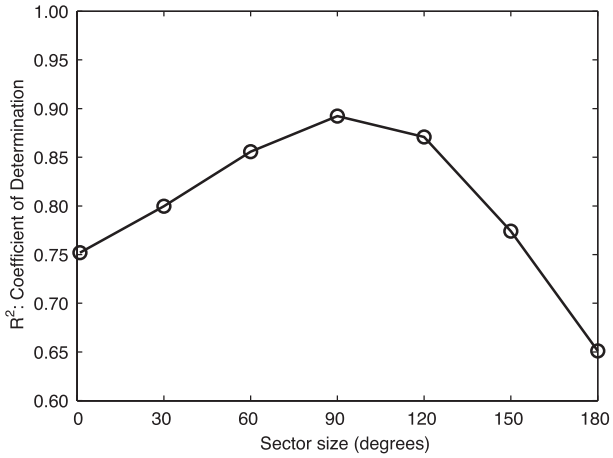

Fig. 20: Variation of R^2 with sector size

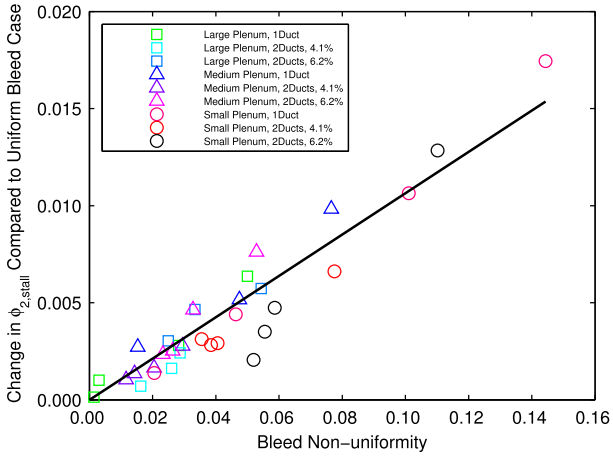

Fig. 21: Change in stage inlet flow coefficient at stall with bleed non-uniformity (evaluated using a 90 degree sector average)

CONCLUSIONS

The following conclusions are drawn from the current work:

1. Non-axisymmetric bleed system geometry, typically caused by a finite number of plenum off-take pipes, creates a non-uniform circumferential distribution of bleed flow extraction from the compressor.
2. Non-uniform bleed creates a static pressure distortion in the main annulus. For the test compressor described in this work, the low static pressure associated with the regions of high bleed causes the flow upstream of the slot to accelerate. Flow is then removed in the bleed slot so that downstream of the slot there remains a flow coefficient deficit at locations of high bleed. For a machine with stages upstream of the bleed, this static pressure distortion would cause the upstream stages to deliver a circumferentially non-uniform total pressure.
3. Whatever configuration of bleed system, the non-uniform distribution of relative flow angle at inlet to the downstream rotor - the incidence variation - determines the impact of the non-uniformity on the stability of the downstream stage. The response of the downstream stage to the varying incidence caused by the non-uniform bleed is analogous to compressors subjected to an inlet total pressure distortion.
4. For the compressor under test, and, we infer, for comparable compressors with similar hub-to-tip radius ratios, the change in flow coefficient at stall between cases with non-uniform bleed and uniform bleed (at the same bleed rate) is

found to correlate with the peak sector-averaged bleed non-uniformity.

ACKNOWLEDGEMENTS

The authors are grateful for the comments and suggestions made by Professor E.M. Greitzer and Dr. T.P. Hynes during the production of this paper. The authors would also like to thank the other members of the Whittle Laboratory, the Gas Turbine Lab at MIT and Mitsubishi Heavy Industries who have provided assistance during the course of the project: Dr. I.J. Day, Dr. J.P. Longley, Professor Z.S. Spakovszky, Dr. S. Aoki, Dr. S. Uchida, R. Mito, J. Iwatani, S. Yamashita.

References

[1] Leishman, B.A. and Cumpsty, N.A. and Denton, J.D., 2007. "Effects of Bleed Rate and Endwall Location on the Aerodynamic Behavior of a Circular Hole Bleed Off-Take". *ASME J. Turbomach., **129***.

[2] Leishman, B.A. and Cumpsty, N.A. and Denton, J.D., 2007. "Effects of Inlet Ramp Surfaces on the Aerodynamic Behavior of Bleed Hole and Bleed Slot Off-Take Configurations". *ASME J. Turbomach., **129***.

[3] Conan, F. and Savarese, S., 2001. "Bleed Airflow CFD Modelling in Aerodynamics Simulations of Jet Engine Compressors". *ASME IGTI Turbo Expo, 2001-GT-544*.

[4] Wellborn, S.R. and Koiro, M., 2002. "Bleed Flow Interactions with an Axial Flow Compressor Powerstream". *AIAA/ASME Joint Propulsion Conference, AIAA 2002-4057*.

[5] Leishman, B.A. and Cumpsty, N.A., 2007. "Mechanism of the Interaction of a Ramped Bleed Slot With the Primary Flow". *ASME J. Turbomach., **129***.

[6] Gomes, R. and Schwarz, C. and Peitzner, M., 2005. "Aerodynamic Investigations of a Compressor Bleed Air Configuration Typical for Aeroengines". *ISABE-2005-1264*.

[7] Gomes, R. and Schwarz, C., 2006. "Experimental Investigation of a Generic Compressor Bleed System". *ASME IGTI Turbo Expo, GT2006-90458*.

[8] Di Mare, L. and Simpson, G. and Mueck, B. and Sayma, A., 2006. "Effect of Bleed Flows on Flutter and Forced Response of Core Compressors". *ASME IGTI Turbo Expo, GT2006-90683*.

[9] Reid, C., 1969. "The Response of Axial Flow Compressors to Intake Flow Distortion". *ASME 69-GT-29*.

[10] Rannie, W.D. and Marble, F.E., 1957. "Unsteady Flows in Axial Turbomachines". *Communication aux Journées Internationales de Sciences Aéronautiques, Paris 27-29 May 1957*.

[11] Greitzer, E.M. and Mazzawy, R.S. and Fulkerson, D.A., 1978. "Flow Field Coupling Between Compression System Components in Asymmetric Flow". *ASME J. Eng. for Power*.

List of figure captions

Fig. 1: Meridional view of test compressor showing measurement planes

Fig. 2: Detail of bleed slot instrumentation

Fig. 3: Rig inlet total-to-static pressure rise characteristic

Fig. 4: Stage inlet total-to-static pressure rise characteristic

Fig. 5: Spanwise distributions of flow coefficient through the compressor at different bleed rates, fixed $\phi_{stage} = 0.43$

Fig. 6: Unsteady casing pressure transducer traces at rotor inlet at stall

Fig. 7: Rig and stage inlet flow coefficient at stall

Fig. 8: Spanwise distribution of rotor inlet relative flow angle, near casing, $\phi_{stage} = 0.38$

Fig. 9: Stage inlet total-to-static pressure rise characteristics for uniform and sample non-uniform bleed

Fig. 10: Variation in local passage-averaged flow coefficient variation with circumferential position, average $\phi_{stage} = 0.38$

Fig. 11: Comparison of bleed distributions measured in slot and derived from traverse data

Fig. 12: Change in passage-averaged flow angle compared to mean value, $\phi_{stage} = 0.38$

Fig. 13: Flow schematic (top) and flow coefficient distributions for isolated bleed extraction with no net main annulus flow

Fig. 14: Flow schematic (top) and flow coefficient distributions for bleed extraction with swirling main annulus flow

Fig. 15: Flow angle at measurement point closest to casing (97.2% span), $\phi_{stage} = 0.38$

Fig. 16: Stage inlet flow coefficient at stall

Fig. 17: Variation in stage inlet flow coefficient at stall with angular separation of off-take ducts (2 duct cases)

Fig. 18: Variation of local bleed rate in slot with circumferential position relative to off-take duct

Fig. 19: Obtaining the peak-sector-averaged bleed non-uniformity

Fig. 20: Variation of R^2 with sector size

Fig. 21: Change in stage inlet flow coefficient at stall with bleed non-uniformity (evaluated using a 90 degree sector average)